Numerical simulation of flow at the vicinity of a hydraulic jump with higher order scheme

Wen Kiat, Ting
River Engineering and Urban
Drainage Research Centre
Universiti Sains Malaysia
Nibong Tebal, Malaysia
wenkiat97@student.usm.my

How Tion, Puay
River Engineering and Urban
Drainage Research Centre
Universiti Sains Malaysia
Nibong Tebal, Malaysia
redac_puay@usm.my

Nor Azazi Zakaria
River Engineering and Urban
Drainage Research Centre
Universiti Sains Malaysia
Nibong Tebal, Malaysia
redac01@usm.my

in

***Abstract*— It is essential to develop a numerical model which could accurately predict the flow depth before and after the hydraulic jump. Therefore, in this study, a numerical model is developed to simulate flow at the vicinity of a hydraulic jump occuring in a straight rectangular open channel. The numerical model consists of a set of one-dimensional depth-averaged continuity and momentum equation. The Constrained Interpolation Profile (CIP) scheme, which is a higher-order numerical scheme, was used to solve the advection term in the governing equations. The numerical model was first verified against the analytical solution of dam-break flow problem of inviscid fluid. Close agreement was observed between the numerical and analytical results. The numerical model was then validated against the experimental data. The flow profile at the location before and after the hydraulic jump structure for flow with Froude number between 2.3 to 7.0 could be reproduced numerically with good accuracy. The location of hydraulic jump could also be predicted by the model.**

Keywords— Depth-averaged equation, Constrained Interpolation Profile (CIP) scheme, Numerical model, Hydraulic jump

I. INTRODUCTION

Hydraulic jump is a rapidly varied phenomenon in open channel flow. Hydraulic jump occurs when the flow changes from supercritical to subcritical state, an abrupt rise of water surface. After the hydraulic jump, flow energy is reduced and flow velocity become stable. Thus, hydraulic jump acts as energy dissipator. This characteristic makes hydraulic jump a good mechanism to be used in various hydraulic structure such as construction of spillway and stilling basin [3].

Hydraulic jump also helps to promote aeration because turbulent flow motion entrapped air bubbles from the air and entrained air bubbles in the water for a longer duration.

In this study, a one-dimensional numerical model is developed to simulate the flow at the vicinity of hydraulic jump in a rectangular channel. The numerical model is coded in FORTRAN 95 programming language. A higher-order numerical scheme (CIP scheme) is used to solve the advection terms in the one-dimensional governing depth-averaged equation: continuity and momentum equations. CIP scheme was developed by Yabe et al. in 1985. CIP is a third order accuracy numerical scheme, in both time and space derivative [6]. Besides that, CIP scheme has been proved to be superior as it can capture discontinuities without severe numerical oscillation. In other words, CIP possesses shock-capturing ability.

In rapidly varied flow with steep water surface gradient, the pressure distribution is non-hydrostatic. Therefore, the inclusion of Boussinesq term to account for the effect of non-hydrostatic pressure is required. However, Chaudhry And Gharangik [2] showed that the Boussinesq term has little effect on numerical reproduction of the location of hydraulic jump. In addition, for flow away from the hydraulic jump, the effect of Boussinesq terms is less significant. Therefore, in this study the Boussinesq term is not included in the model.

The numerical model is first verified against the Ritter's solution which is the analytical solution for the one-dimensional dam-break flow problem. The existence of discontinuity at the flow front in dam-break flow problem served as a convenient target for numerical studies [4]. Validation of the numerical model is carried out to ensure that the model could reproduce experimental results [5].

II. METHODOLOGY

A. Experimental Setup

The experimental setup is referred to the paper published by Chaudhry and Gharangik [2]. To avoid confusion, we need to clarify that we did not carry out any physical experiment and the experimental result used in the validation of the numerical model is obtained from Chaudhry and Gharangik [2]. In their paper, the experimental facilities compromise of a rectangular metal flume with dimension: 14.0 m long, 0.915 m high, and 0.46 m wide, a sharp-edged sluice gate at the upstream and an adjustable downstream tailgate. These experimental facilities are shown in Figure 1. The dimension of the flume, inflow condition and outflow condition of the experiment were taken as a reference to simulate the same condition for comparison purpose.

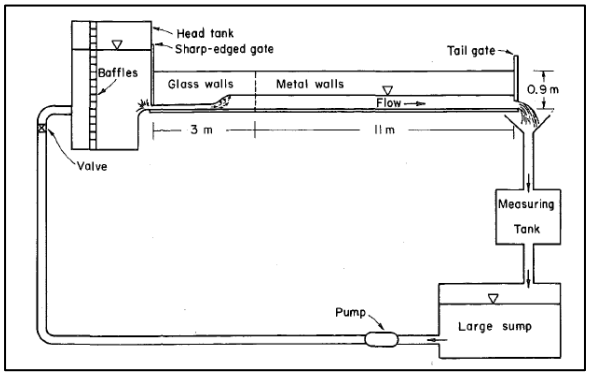

Fig. 1. Experimental facilities by Chaudhry and Gharangik [2]

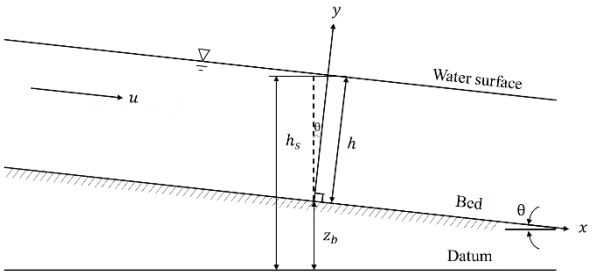

Fig. 2. Definition of flow variables in the one-dimensional depth-averaged model

B. Development of numerical model

The governing equations solved in the numerical model are the depth-averaged continuity and momentum equations shown in Eq. 1 and Eq. 2 respectively. The flow variables in the governing equation are defined based on Figure 2.

$$\frac{\partial h}{\partial t} + \frac{\partial (uh)}{\partial x} = 0 \tag{1}$$

$$\frac{\partial (uh)}{\partial t} + \frac{\partial (uuh)}{\partial x} = -gA\left(\frac{\partial h_s}{\partial x} + \frac{\tau_{bx}}{\rho g R}\right) \tag{2}$$

Here, u= depth-averaged velocity in x-direction, h_s= water surface elevation and h= flow depth. A is the cross-sectional area of flow defined as Bh for rectangular channel where B is the width of the channel, τ_{bx}= bottom shear stress in x-direction, g= gravity acceleration, R = hydraulic radius and ρ = density of water. The definition of the flow variables and coordinate setup for the problem is shown in Figure 1 where h_s is defined as $h_s = h(x,t)\ cos\ \theta + z_b$ and z_b= bed elevation from the datum.

C. Solution Algorithm

The conservative form of the continuity and momentum equation are changed into a non-conservative form as shown in Eq. 3 and Eq. 4. CIP scheme are only used to solve the advection form on the left-hand side of Eq. 3 and Eq. 4.

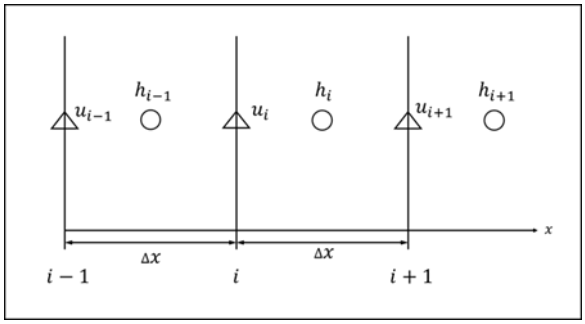

Fig. 3. Staggered grid system used to define the location of flow variables used in the numerical model

$$\frac{\partial h}{\partial t} + u\frac{\partial h}{\partial x} = -h\frac{\partial u}{\partial x} \tag{3}$$

$$\frac{\partial u}{\partial t} + u\frac{\partial u}{\partial x} = -g\frac{\partial h}{\partial x} \tag{4}$$

Time-splitting method [9] is used to solve Eq. 3 and Eq.4 in two parts, i.e. the advection part (left-hand side) and the non-advection part (right-hand side).

Step 1

The advection part of the continuity and momentum equations are shown in Eq. 5 and Eq. 6. The value of h and u are upgraded to temporary values ($h*$ and $u*$) after solving the advection terms with CIP schemes.

$$\frac{\partial h}{\partial t} + u\frac{\partial h}{\partial x} = 0 \xrightarrow{solved\ with\ CIP} \therefore h^n \to h^* \tag{5}$$

$$\frac{\partial u}{\partial t} + u\frac{\partial u}{\partial x} = 0 \xrightarrow{solved\ with\ CIP} \therefore u^n \to u^* \tag{6}$$

Step 2

After solving the advection term, the non-advection term can be solved by using Eq. 7 and Eq. 8 which are cast from Eq. 3 and Eq. 4.

$$\frac{\partial h}{\partial t} = -h\frac{\partial u}{\partial x} \tag{7}$$

$$\frac{\partial u}{\partial t} = -g\frac{\partial h}{\partial x} \tag{8}$$

Eq. 7 and Eq. 8 are discretized using finite difference method as in Eq. 9 and Eq. 10 (based on staggered grid system shown in Figure 3).

$$\frac{h_i^{n+1} - h_i^*}{\Delta t} = -h_i^*\frac{u_{i+1}^{n+1} - u_i^{n+1}}{\Delta x} \tag{9}$$

$$\frac{u_i^{n+1} - u_i^*}{\Delta t} = -g\frac{\partial h^{n+1}}{\partial x} \tag{10}$$

Since the calculation of new value of h which is represented by h^{n+1} in Eq. 9 requires the new value of u which is represented by u^{n+1} and the value of u^{n+1} depends on the value of h^{n+1} in Eq. 10, it is obvious that the h^{n+1} has to be solved implicitly. The method to solve for h^{n+1} and u^{n+1} is based on the SMAC (Simplified Market and Cell) method [7] and explained based on Kawasaki et al. [8] as follows:

First, an initial guess for $u^{n+1}$is made by using the temporary value h for the term $\frac{\partial h^{n+1}}{\partial x}$. The initial guess is labelled as $\tilde{u}_i$ as follows:

$$\tilde{u}_i = u_i^* - g\Delta t \frac{\partial h_i^*}{\partial x} \quad (11)$$

Eq. 11 is then subtracted by Eq. 10 to obtain the following relations:

$$\frac{u_i^{n+1} - \tilde{u}}{\Delta t} = -g \frac{\partial}{\partial x}(\delta h)_i \quad (12)$$

$$(\delta h)_i = h_i^{n+1} - h_i^* \quad (13)$$

Eq. 12 and Eq.13 are then substituted into Eq. 9 to obtain a Poisson equation shown in Eq. 14.

$$\frac{\partial^2 (\delta h)_i}{\partial x^2} = \frac{1}{g\Delta t}\left(\frac{\partial \tilde{u}}{\partial x} + \frac{(\delta h)_i}{\Delta t . h_i^*}\right) \quad (14)$$

The discretization of the Poisson equation is shown in Eq. 15.

$$\frac{\delta h_{i+1} + \delta h_{i-1} - 2\delta h_i}{(\Delta x)^2} = \frac{1}{g\Delta t}\left(\frac{\tilde{u}_{i+1} - \tilde{u}_i}{\Delta x} + \frac{(\delta h)_i}{\Delta t . h_i^*}\right) \quad (15)$$

Eq. 15 is solved with SOR (Successive Over Relaxation) method with the over relaxation factor of 1.6 to obtain $(\delta h)_i$.

Step 3

The new value of h and u is updated based on Eq. 12 and Eq. 13 as shown in Eq. 16 and Eq. 17.

$$h_i^{n+1} = h_i^* + (\delta h)_i \quad (16)$$

$$u_i^{n+1} = \tilde{u}_i - g\Delta t\left(\frac{\delta h_i - \delta h_{i-1}}{\Delta x}\right) \quad (17)$$

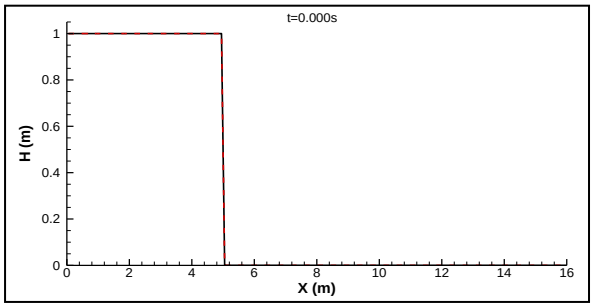

Fig. 4. Initial condition of dam-break flow problem

D. Verification of numerical model

Numerical model is used to simulate one-dimensional dam-break flow problem. The simulation results obtained from the numerical model are compared with Ritter's solution. Ritter's solution is an analytical solution for wave structure in a sudden dam break of flow propagating from a dam reservoir to a dry downstream channel bed [1]. Assumptions for this solution are as follows: perfect fluid is used, and the horizontal bed is assumed to be flat. Therefore, the bottom shear stress term, $\frac{\tau_b}{\rho g R}$ is neglected and the bed slope is equal to zero (z_b=0). The initial condition for the simulation of dam-break flow is shown in Figure 4. In the simulation, time increment, Δt = 0.001s and cell size, Δx = 0.1m are used.

E. Validation of numerical model

The one-dimensional numerical model is used to simulate hydraulic jump problem to evaluate the performance of the model in reproducing the flow profile at the vicinity of the hydraulic jump. Here, a flat channel bottom is assumed, therefore $z_b = 0$. Besides that, the bottom shear stress term $\frac{\tau_{bx}}{\rho g R}$ is evaluated in the model by using Manning's n as follows,

$$\frac{\tau_{bx}}{\rho g R} = \frac{u|u|n^2}{h^{4/3}} \quad (18)$$

where n is the Manning's roughness coefficient.

The numerical simulation result is then compared with numerical result and experimental data carried out by Chaudhry and Gharangik [2]. The initial condition for the simulation of hydraulic jump is shown in Figure 5. In the simulation, time increment, Δt = 0.001s and cell size, Δx = 0.1m are used. 6 cases of Froude number (based on Chaudhry and Gharangik [2] experiment) are used to simulate the hydraulic jump problem and the simulation conditions of the hydraulic jump problem are shown in Table 1.

TABLE I. SIMULATION CONDITIONS OF THE HYDRAULIC JUMP PROBLEM BASED ON DIFFERENT EXPERIMENT CASES CARRIED OUT BY CHAUDHRY AND GHARANGIK [2]

Case	Froude number, Fr	Manning's Roughness, n	Inflow depth, h_1 (m)	Outflow depth, h_2 (m)
1	2.3	0.014	0.064	0.168
2	2.9	0.016	0.055	0.189
3	4.23	0.020	0.043	0.222
4	5.74	0.022	0.040	0.286
5	6.65	0.022	0.024	0.195
6	7.0	0.020	0.031	0.265

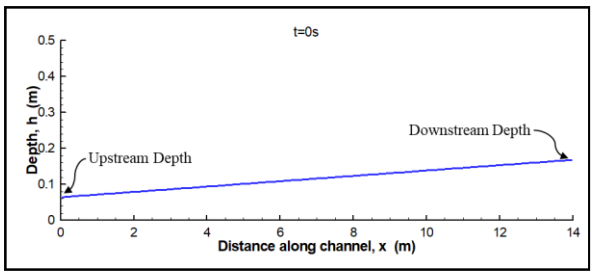

Fig. 5. Initial condition of hydraulic jump problem

III. RESULT AND DISCUSSION

A. *Verification of numerical model*

The result for the simulation of one-dimensional dam-break flow problem are shown in Figure 6. As shown in Figure 6, the speed of the leading wave agrees with Ritter's solution. The negative wave propagating towards the upstream wall is also well reproduced in the numerical model. In addition, numerical oscillations are not observed at the discontinuities at the front wave. Hence, it can be said that the model was well verified against the Ritter's solution.

B. *Validation of numerical model*

The hydraulic jump problem for the 6 cases of Froude number were simulated. The results of the steady-state flow profile for the respective case are shown from Figure 7 to Figure 12. The overall flow profile reproduced by the numerical model shows good agreement with the experimental data by Chaudhry and Gharangik[2] especially at the regions away from the hydraulic jump. This is because vertical acceleration is negligible at these regions.

The model overpredicted the surface gradient of the hydraulic jump in all the cases especially for steady jump cases in Case 4, 5 and 6 where the Froude number is larger than Fr=4.5 [10]. On the other hand, the location of hydraulic jump was well reproduced by the model despite the absence of Boussinesq term in the numerical model. Hence, it can be said that Boussinesq term has little effect in determining the location of the hydraulic jump.

Therefore, the steady-state flow profile that the numerical model is able to reproduce an accurate prediction of flow profile at the location before and after hydraulic jump for flow with Froude number from 2.3 to 7.0. It is also worth to note that height of the hydraulic jump increases as the Froude number increases. Hence, it can be said that the numerical model is reliable to reproduce the formation of hydraulic jump.

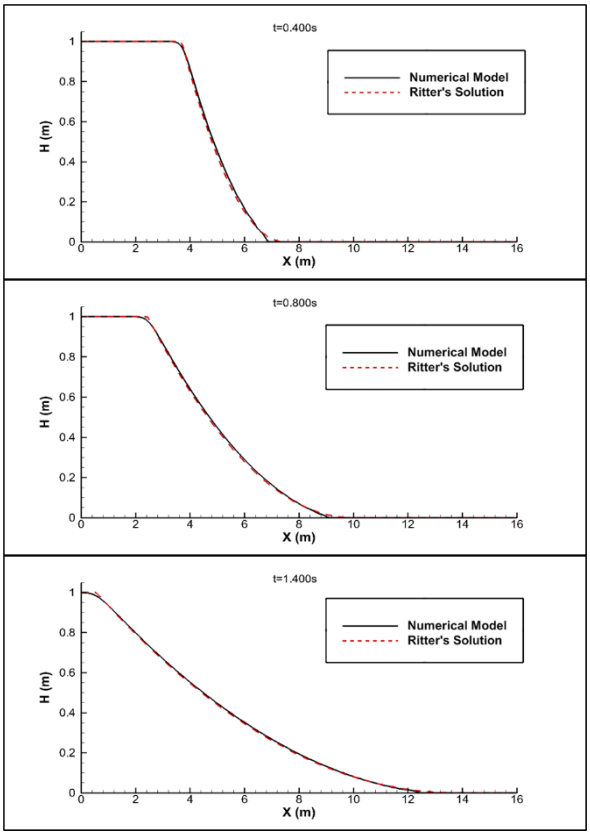

Fig. 6. Simulation of one-dimensional dam-break flow problem from t = 0.0 s to t = 1.4 s

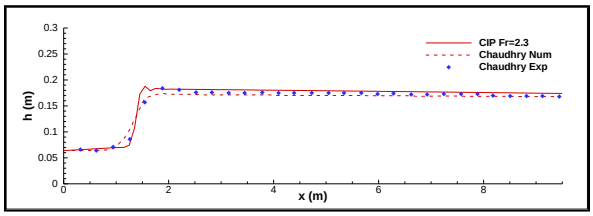

Fig. 7. Flow profile for Case 1 (Fr=2.3) at steady state (t = 70.0 s)

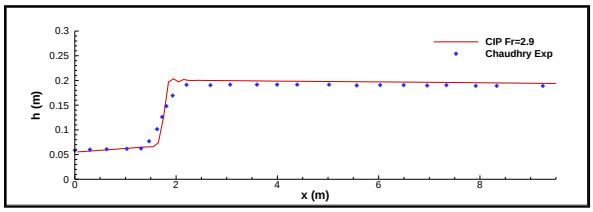

Fig. 8. Flow profile for Case 2 (Fr=2.9) at steady state (t = 70.0 s)

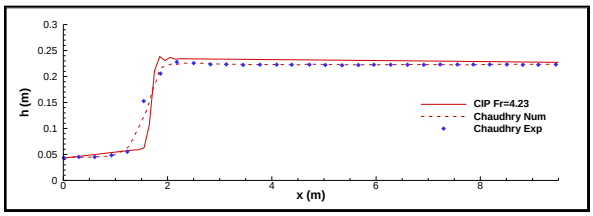

Fig. 9. Flow profile for Case 3 (Fr=4.23) at steady state (t = 70.0 s)

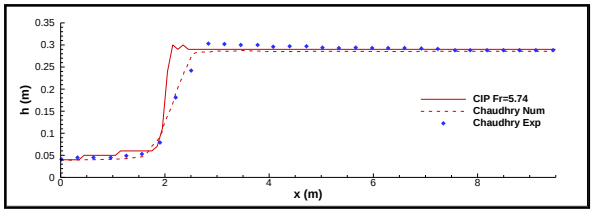

Fig. 10. Flow profile for Case 4 (Fr=5.74) at steady state (t = 70.0 s)

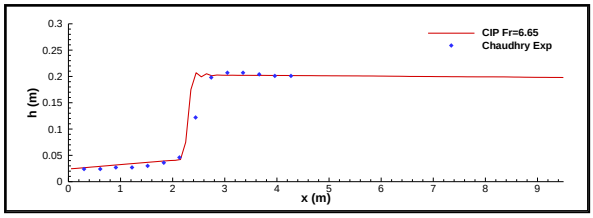

Fig. 11. Flow profile for Case 5 (Fr=6.65) at steady state (t= 70.0 s)

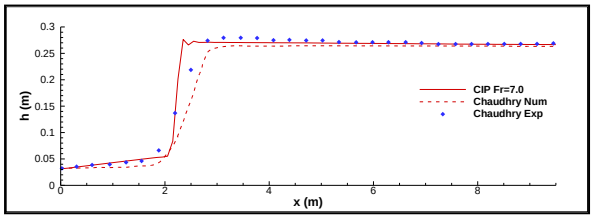

Fig. 12. Flow profile for Case 6 (Fr=7.0) at steady state (t = 70.0 s)

IV. CONCLUSION

A higher order one-dimensional depth-averaged model was developed in this study. The CIP scheme, which is a third order accuracy scheme was used to solve the advection terms in the depth-averaged equation.

The numerical model was first verified against Ritter's solution. A close agreement was observed between the result of numerical model and Ritter's solution.

In the validation process, the numerical model was validated against the experiment and numerical simulation of hydraulic jump. It was shown that the numerical model developed in this study could reproduce flow profile at the location before and after hydraulic jump with good accuracy. Hence, it can be said that the numerical model has good accuracy in reproducing the flow at the vicinity of the hydraulic jump and the location of the hydraulic jump could be predicted well by the model.

REFERENCES

[1] O. Castro-Orgaz and H. Chanson, Ritter's dry-bed dam-break flows: positive and negative wave dynamics. Environmental Fluid Mechanics, 2017.

[2] M. H. Chaudhry and A. M. Gharangik, Numerical Simulation of Hydraulic Jump. Journal of Hydraulic Engineering, vol. 117(9), pp.1195-1211, 1994.

[3] W. H. Hager, Energy Dissipaters and Hydraulic Jump. Dordrecht: Kluwer Academic Publishers, 1995.

[4] Q. Ji, X. Zhao, and S. Dong, Numerical Study of Violent Impact Flow Using a CIP-Based Model. Journal of Applied Mathematics, 2013.

[5] W. L. Oberkampf and T. G. Trucano, Verification and validation in computational fluid dynamics. Progress in Aerospace Sciences, 38, pp.209-272, 2002.

[6] T. Yabe, H. Mizoe, K. Takizawa, H. Moriki, H. N. Im and Y. Ogata, Higher-order schemes with CIP method and adaptive Soroban grid towards mesh-free scheme. Journal of Computational Physics, 194, pp.57-77, 2004.

[7] A. A. Amsden and F. H. Harlow, A simplified MAC technique for incompressible fluid flow calculations. Journal of computational physics, 6(2), 322-325, 1970.

[8] K. Kawasaki, T. ONO, P. Piamsa-nga, H. Atsuta and K. Nakatsuji, Development of depth-averaged inundation flow model based on CIP method and SMAC method, Journal of Hydraulic JSCE, 48, pp. 565-570, 2004 (in Japanese).

[9] T. Yabe and Takei. E, A new higher-order Godunov method for general hyperbolic equations. Journal of the Physical Society of Japan, 57, 2598-2601, 1988

[10] V. T. Chow, Open-channel hydraulics. McGraw-Hill civil engineering series, 1959.